

# Single-atom lasing induced atomic self trapping

Thomas Salzburger and Helmut Ritsch

*Institute for Theoretical Physics, University Innsbruck, A 6020 Innsbruck, Austria*

We study motion and field dynamics of a single-atom laser consisting of a single incoherently pumped free atom moving in an optical high- $Q$  resonator. For sufficient pumping, the system starts lasing whenever the atom is close to a field antinode. If the field mode eigenfrequency is larger than the atomic transition frequency, the generated laser light attracts the atom to the field antinode and cools its motion. Using quantum Monte Carlo wave function simulations, we investigate this coupled atom-field dynamics including photon recoil and cavity decay. In the regime of strong coupling, the generated field shows strong nonclassical features like photon antibunching, and the atom is spatially confined and cooled to sub-Doppler temperatures.

PACS numbers: 32.80.Pj, 42.50.Vk, 42.50.Lc

Optical cavity QED experiments using high finesse resonators and ultracold neutral atoms have seen tremendous progress towards larger coupling strength and interaction time in the past decade, becoming a fruitful test ground of quantum theory [1, 2, 3, 4, 5]. One particular goal of cavity QED is a single-atom, single-mode laser. In analogy to the micromaser, a one atom laser using an atomic beam crossing an optical resonator has been realized some time ago [6]. However, although effectively only a single or a few atoms are present at a time, the short interaction times make this still a many particle device. Very recently important progress towards single particle lasing has been achieved by placing a small ion trap into a high- $Q$  cavity [2, 7]. This allows very long interaction times, but technical limits set by the ion trap still prevent to reach threshold.

In all optical setups the atoms are extremely cold at the beginning, but the light forces induced by the cavity field and pumping itself lead to fast heating. Even less than a single photon on average induces significant dissipation [1] and limits interaction times. By a proper choice of parameters, one can minimize this heating caused by light forces [8] or even use cavity induced cooling forces [9, 10] to enlarge the trapping times. Alternatively, the addition of an extra dipole trapping potential led to much larger interaction times [11] and enabled the first realization of single atom lasing in the strong coupling regime [5]. Here, steady state light output generated from one atom for almost a second was achieved from a three photon Raman type gain scheme.

In this Letter we go conceptually one step beyond and assume that no coherent field is applied to the atom or the mode and no extra atom trap is present. The cavity field is entirely generated by gain from the incoherently pumped atom. Neglecting atomic motion, such single atom laser models have been widely used in fundamental studies of quantum laser theory [12]. They constitute light sources with unique properties. For example, one is able to sustain a stationary single photon Fock state or generate highly sub-Poissonian output [13]. Note that the same single atom is present during the whole time

here.

Extending these models, we include the atomic motion governed by the light forces of the laser field created by the atom itself. As expected, the proper accounting of the cavity field forces implies significant modifications of the system dynamics [9]. In general, the atomic motional variables and the dynamics of the internal variables are coupled and correlated or even entangled. The atom moves under the influence of the dipole force which depends on the mode intensity. This intensity in turn depends on the atomic position in a highly nonlinear way as the atom itself is the gain medium.

From a first guess, one could already expect some self-trapping effect if one chooses the parameters such that lasing only starts when the atom is close to a field antinode. The laser field then could generate an attractive potential keeping the atom in the vicinity of this antinode. Naively, this requires the lasing mode to be red detuned relative to the atomic transition frequency. In this case, though, the extra energy from the atomic transition is likely to be converted into kinetic energy heating the atom. Similarly, for a blue detuned cavity mode, one expects cooling but repulsion from the antinodes. However, the situation is a bit more complicated. As gain requires atomic inversion, an atom in steady state can still be a high field seeker for blue detuning, and the laser frequency is itself a dynamical quantity. Thus, we can still hope to find parameters where trapping, cooling, and lasing coincide. Of course, heating through spontaneous emission and dipole fluctuations will also be present. This makes the total dynamics hard to guess, which motivated us to study the problem in more detail.

Let us now define our model as simple as possible still containing the essential physics. For this we restrict ourselves to a two-level atom moving in a single strongly coupled cavity mode in one dimension. As in well proven approaches developed in the early days of laser theory [12], incoherent pumping can be consistently modelled by inverse spontaneous emission at rate  $2\delta$ . Following standard procedures of quantum optics, we can derive the master equation  $\dot{\rho} = \mathcal{L}\rho$  governing the time evolution of

field and atom including atomic spontaneous emission at rate  $2\gamma$  and cavity decay at rate  $2\kappa$ .

In a frame rotating at the mode frequency  $\omega_c$  we get:

$$\begin{aligned} \mathcal{L}\rho = & i\Delta \left[ |e\rangle\langle e|, \rho \right]_- - g \cos(kx) \left( \left[ |e\rangle\langle g|a, \rho \right]_- - \left[ a^\dagger|g\rangle\langle e|, \rho \right]_- \right) \\ & + \delta \left( 2|e\rangle\langle g|\rho|g\rangle\langle e| - \left[ |g\rangle\langle g|, \rho \right]_+ \right) + \gamma \left( 2|g\rangle\langle e|\rho|e\rangle\langle g| - \left[ |e\rangle\langle e|, \rho \right]_+ \right) + \kappa \left( 2a\rho a^\dagger - \left[ a^\dagger a, \rho \right]_+ \right). \end{aligned} \quad (1)$$

Here  $|g\rangle$  ( $|e\rangle$ ) and  $a$  denote the atomic ground (excited) state and the field annihilation operator, respectively. The cavity mode with mode function  $\cos(kx)$  and frequency  $\omega_c$  is detuned from the atomic transition frequency  $\omega_a$  by  $\Delta = \omega_c - \omega_a$ .

In a first step we look at the steady state of the system for fixed atomic position  $x$  which enters the equations only via the coupling strength  $g \cos(kx)$ . In Fig. 1 we plot the photon number  $\bar{n}$  (solid line), its scaled uncertainty  $\Delta_n/\bar{n}$  (dashed), and the atomic upper state population (dash-dotted) as a function of  $g$  for fixed pump strength  $\delta = 75\kappa = 7.5\gamma$  for large atom-field detuning  $\Delta = 250\kappa$ . As expected, the photon number depends upon  $g$  in a nonlinear way and the system starts lasing only for sufficiently large  $g$  when the atom is close to a field antinode. With growing photon number ( $\bar{n} > 1$ ) the corresponding spectrum shown in the little inserts of Fig. 1 is blue shifted from the atomic resonance and acquires a width below the empty cavity linewidth. Hence, we can hope for stable trapping close to the antinode combined with lasing at these parameters.

Let us include atomic motion and check. Since the number of degrees of freedom is rather large now, we use a Monte Carlo wave function simulation technique to numerically approximate the solution of the master

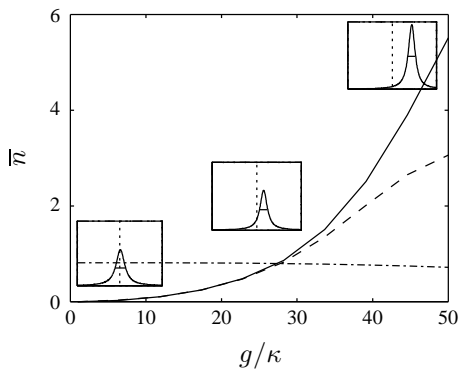


FIG. 1: Average photon number  $\bar{n}$ , scaled uncertainty  $\Delta_n/\bar{n}$ , and upper state population as function of  $g/\kappa$ . The parameters are  $(\gamma, \delta, \Delta) = (10\kappa, 75\kappa, 250\kappa)$ . The little inserts show the emitted light spectrum for  $g = (5, 25, 45)\kappa$ .

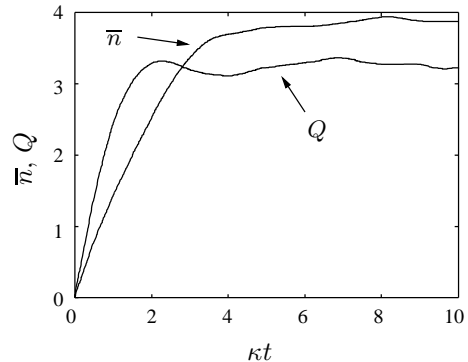


FIG. 2: Average photon number  $\bar{n}$  and Mandel  $Q$  parameter for the lasing startup phase. The parameters are  $(\gamma, \delta, g) = (10\kappa, 60\kappa, 50\kappa)$  where the cavity field is detuned from the atomic transition by  $\Delta = 250\kappa$ .

equation [15]. Averaging gives an approximate density operator  $\rho(t)$  while analyzing individual trajectories provides extra insight in the microscopical dynamics.

We briefly review the method now. Defining a super-operator  $\mathcal{S}\rho = \sum_i \hat{C}_i \rho \hat{C}_i^\dagger$  based on collapse operators  $\hat{C}_i$  related to the quantum jumps, we get single trajectories by propagation with a non-hermitian Hamiltonian  $H_{\text{eff}}$

$$(\mathcal{L} - \mathcal{S})\rho = -iH_{\text{eff}}\rho + i\rho H_{\text{eff}}^\dagger, \quad (2)$$

in between stochastically occurring jumps. The jump probabilities within the interval  $[t, t + \Delta t]$  are given by  $p_i(t) = \langle \psi(t) | \hat{C}_i^\dagger \hat{C}_i | \psi(t) \rangle \Delta t$ . One first propagates  $|\psi(t)\rangle$  using  $H_{\text{eff}}$  for one time step  $\Delta t$

$$|\psi(t + \Delta t)\rangle = \exp(-iH_{\text{eff}}\Delta t)|\psi(t)\rangle \quad (3)$$

and calculates  $p_i$ . Using random numbers  $r_i \in [0, 1]$  and comparing them to  $p_i(t)$ , one then decides on the occurrence of collapses  $|\psi\rangle \rightarrow \hat{C}_i|\psi\rangle$  at the end of  $\Delta t$ . The jumps here include atomic decay ( $\sqrt{2\gamma}|g\rangle\langle e|$ ), cavity decay ( $\sqrt{2\kappa}a$ ), and pump events ( $\sqrt{2\delta}|e\rangle\langle g|$ ).

Explicitly the effective Hamiltonian  $H_{\text{eff}}$  reads ( $\hbar = 1$ )

$$\begin{aligned} H_{\text{eff}} = & -i\delta|g\rangle\langle g| - (\Delta + i\gamma)|e\rangle\langle e| - i\kappa a^\dagger a \\ & - ig \cos(kx) (|e\rangle\langle g|a - a^\dagger|g\rangle\langle e|). \end{aligned} \quad (4)$$

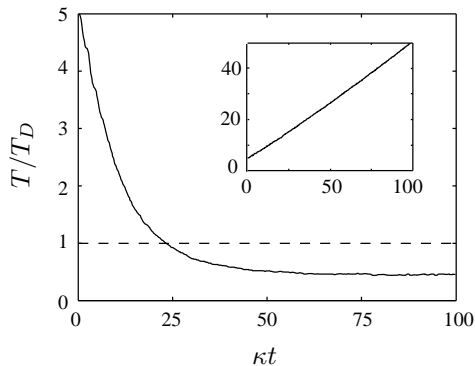


FIG. 3: Mean square velocity in units of the Doppler temperature  $T_D$  for  $\Delta = 250\kappa$ . The other parameters are  $(\gamma, \delta, g) = (10\kappa, 60\kappa, 50\kappa)$ ,  $T_D$  is indicated by the dashed line. For negative detuning the atom gets heated up, see inset where  $\Delta = -250\kappa$ .

As the atomic temperature is well above the recoil limit, we treat the external atomic variables  $x$  and  $p$  classically [14]. Thus we have  $\dot{x} = p/m$  and  $\dot{p} = F$  to add to our equations. The force  $F$  is given by

$$F = \langle \psi | -\frac{\partial H_{\text{eff}}}{\partial x} | \psi \rangle = -i\hbar k \sin kx \langle \psi | e \rangle \langle g | a | \psi \rangle + \text{h.c.} \quad (5)$$

Finally, we have to truncate the Hilbert space  $\mathcal{H} = \text{span}\{|g\rangle, |e\rangle\} \otimes \mathcal{H}_F$  ( $\mathcal{H}_F$  is the Fock-space of the mode) at photon number  $N$ . Our state space thus contains the ground state  $|g, 0\rangle$  and  $N$  manifolds separated by  $\omega_a$  with states  $|g, n\rangle$  and  $|e, n-1\rangle$ ,  $n = 1 \dots N$ . Any wave function is determined by  $2N + 1$  complex numbers,

$$|\psi\rangle = g_0|g, 0\rangle + \sum_{n=1}^N (g_n|g, n\rangle + e_n|e, n-1\rangle), \quad (6)$$

where only  $2N$  are independent due to normalization. Note that in contrast to most previous treatments of light forces in a cavity, we cannot adiabatically eliminate the excited state since we have to deal with an inverted atom.

Let us now examine stochastic simulation averages for typical cases. After turning on the pump, the mean photon number  $\bar{n}$  increases rapidly and reaches a constant value within a few cavity relaxation times (Fig. 2). At the same time the atom gets trapped and remains captured in the potential of the light it has generated. In addition we show the Mandel  $Q$  parameter ( $Q = (\bar{n}^2 - \bar{n})/(\bar{n}) - 1$ ) as a measure of the field intensity noise.

Fig. 3 shows the atomic kinetic energy averaged over 4000 realizations in units of the Doppler temperature  $T_D = \hbar\gamma/2$  for the parameters of Fig. 2 where the mean photon number reaches  $\bar{n} = 3.8$ . Starting at a very low velocity, the atom gets cooled (heated) for a wide range of positive (negative) detunings  $\Delta$ . The inset shows the analogous result for  $\Delta = -250\kappa$ . This agrees with a simple energy conservation argument. The atom gains the

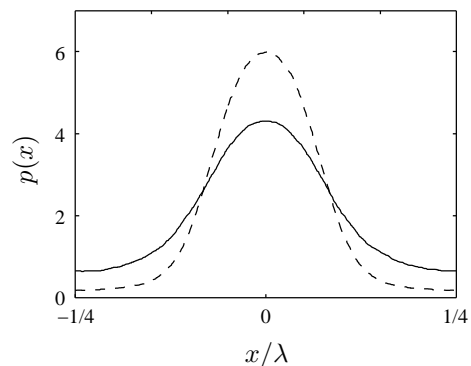


FIG. 4: Position distribution of an atom trapped at an antinode for the parameters of Fig. 3 (solid line) and for a larger pumping rate  $\delta = 80\kappa$  (dashed line).

internal energy  $\hbar\omega_a$  from a pump event. Subsequently it loses the energy  $\hbar\omega_c$  by stimulated emission into the cavity mode. The energy mismatch is compensated by the atomic center of mass motion which gets damped if  $\omega_c - \omega_a > 0$ . This argument is confirmed by a closer look at basic absorption and emission processes including Doppler shift from the atomic motion.

Naively one would guess that the atom is expelled from the interaction region of a blue shifted light field. However, this is not true for a partially inverted atom which still can be trapped near the mode antinodes. This feature is essential to allow steady state operation of our single-atom laser. The solid line in Fig. 4 shows the position distribution of an atom trapped after the cooling process of Fig. 3. Clearly, the atom spends most of the time in the vicinity of an antinode with a mean square distance of  $\overline{x^2} = (0.1\lambda)^2$ . This value decreases further for larger photon numbers. For  $\bar{n} \approx 12$  (dashed line) we get  $\overline{x^2} = (0.07\lambda)^2$  for a pump strength of  $\delta = 80\kappa$ . The non-vanishing probability near  $x \approx \pm\lambda/4$  shows some remaining hopping of the atom between different trapping sites.

So far we calculated ensemble averages to investigate the motional characteristics. It is now quite interesting to look at individual trajectories  $|\psi(t)\rangle$  to visualize the microscopic dynamics. Fig. 5a depicts a typical example of the photon number time evolution  $\langle n \rangle$  for a trapped atom for ten cavity relaxation times. Starting in a certain state  $|e, n\rangle$ , the system gets entangled with  $|g, n+1\rangle$  owing to the atom-cavity coupling. The incoherent pumping projects it into the state  $|e, n+1\rangle$  and creates a Fock state with  $n+1$  photons. Unless a photon leaks out of the cavity or another one is created, the photonic state remains nearly unchanged for the following reasons. First, we chose a large detuning  $\Delta = 250\kappa$  in order to keep the atom trapped at antinodes as good as possible. Second, the atom undergoes several jumps due to alternating spontaneous emission and pump events. After each of these cycles the system is again projected

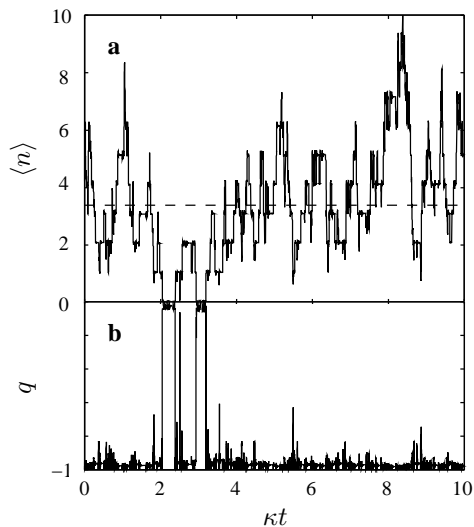


FIG. 5: **a** Photon number expectation value  $\langle n \rangle$  for a single trajectory of a trapped atom within ten cavity relaxation times. The parameters are as in Fig. 3. The dashed line indicates the mean photon number. **b** Corresponding single-trajectory  $q$  factor.

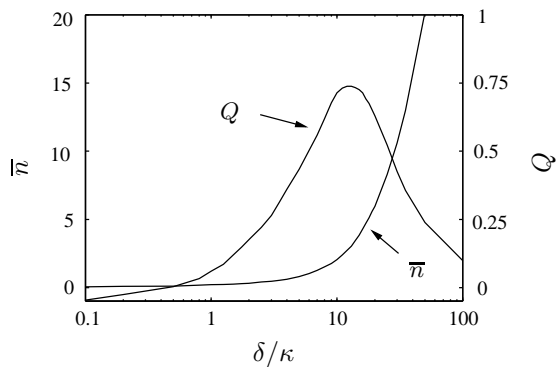


FIG. 6: Mean photon number and Mandel parameter vs pumping strength  $\delta$ .

into the initial state  $|e, n + 1\rangle$ , which gives the cascade shape of the photon number time evolution. Notice that the pumping process creates no coherence, as it would be e.g. in a lambda type system such as in [13]. Here ac Stark splitting of dressed states does not effect the probability of exciting the system which is solely given by the atomic ground state population and, hence, the system can be excited into states with higher photon numbers more easily. Nevertheless, for each trajectory the cavity field remains close to a Fock state with photon numbers varying around the mean value indicated by the dashed line. This behavior is demonstrated in Fig. 5b where the single trajectory Mandel factor – which describes the actual state of the cavity field – attains values close to  $q = -1$  as long as one photon is present at least. This is due to the fact that in each trajectory we know the

number of pump and decay events. Statistical averaging over the pump events washes out this feature.

Let us now come back to ensemble averages of field properties. Fig. 6 depicts  $\bar{n}$  and  $Q$  as a function of  $\delta$  with  $(\Delta, g) = (200\kappa, 100\kappa)$  for  $\gamma = 0$ . In general the field intensity is strongly fluctuating. These fluctuations are even more pronounced than for an atom at rest and in turn increase motional heating. Only for larger photon numbers the Mandel  $Q$  parameter drops down to zero as for a coherent state (lasing).

In summary light forces significantly influence the dynamics of a single-atom laser. Surprisingly, for blue atom-field detuning several effects work together in a favorable way to facilitate steady state lasing in conjunction with mechanical cooling and trapping. Steady state temperatures below the Doppler limit are possible in spite of enhanced momentum diffusion due to fluctuations of the photon number. The light field shows nonclassical features and approximates a coherent state with a coherence time beyond the cavity lifetime only far above threshold. Although the description of the atom is oversimplified here, we believe that our central findings like enhanced trapping and self cooling with lasing still should be present in a real system.

This work was supported by the Austrian FWF under contract S1512. The authors thank P. Domokos and A. Kuhn for helpful discussions.

- 
- [1] P. W. H. Pinkse *et al.*, Nature **404**, 365 (2000); C. J. Hood *et al.*, Science **287**, 1447 (2000).
  - [2] G. R. Guthörlein *et al.*, Nature **414**, 49 (2001); A. B. Mundt *et al.*, Phys. Rev. Lett. **89**, 103001 (2002).
  - [3] J. A. Sauer *et al.*, quant-ph/0309052 (2002).
  - [4] A. Kuhn, M. Henrich, and G. Rempe, Phys. Rev. Lett. **89**, 067901 (2002).
  - [5] J. McKeever *et al.*, Nature **425**, 268 (2003).
  - [6] K. An *et al.*, Phys. Rev. Lett. **73**, 3375 (1994).
  - [7] G. M. Meyer, H.-J. Briegel, and H. Walther, Europhys. Lett. **37**, 317 (1997).
  - [8] A. C. Doherty *et al.*, Phys. Rev. A **63**, 013401 (2001).
  - [9] P. Domokos and H. Ritsch, J. Opt. Soc. Am. B **20**, 1098 (2003).
  - [10] P. Horak *et al.*, Phys. Rev. Lett. **79**, 4974 (1997).
  - [11] J. McKeever *et al.*, Phys. Rev. Lett. **90**, 133602 (2003).
  - [12] H. Haken, *Laser Theory* (Springer, Berlin, 1984); C. Ginzler *et al.*, Phys. Rev. A **48**, 732 (1993).
  - [13] T. Pellizzari and H. Ritsch, Phys. Rev. Lett. **79**, 3973 (1994); H. Ritsch *et al.*, Phys. Rev. A **44**, 3361 (1991).
  - [14] P. Domokos, P. Horak, and H. Ritsch, J. Phys. B: At. Mol. Opt. Phys. **34**, 187 (2001).
  - [15] H. J. Carmichael, *An Open System Approach to Quantum Optics* (Springer, Berlin, 1993); R. Dum, P. Zoller, and H. Ritsch, Phys. Rev. A **45**, 4879 (1992); J. Dalibard and Y. Castin, Phys. Rev. Lett. **68**, 580 (1992).